

2021-03-09

Piezoresistive modelling of CNTs reinforced composites under mechanical loadings

Fang, Y

<http://hdl.handle.net/10026.1/16931>

10.1016/j.compscitech.2021.108757

Composites Science and Technology

Elsevier BV

All content in PEARL is protected by copyright law. Author manuscripts are made available in accordance with publisher policies. Please cite only the published version using the details provided on the item record or document. In the absence of an open licence (e.g. Creative Commons), permissions for further reuse of content should be sought from the publisher or author.

Piezoresistive modelling of CNTs reinforced composites under mechanical loadings

Yuan Fang¹, Long-Yuan Li^{2*}, Sung-Hwan Jang^{3*}

1) Guangdong Provincial Key Laboratory of Durability for Marine Civil Engineering, Shenzhen University, Shenzhen 518060, P R China (yuanfang@szu.edu.cn)

2) School of Engineering, Computing and Mathematics, University of Plymouth, Plymouth, Devon PL4 8AA, UK (long-yuan.li@plymouth.ac.uk)

3) School of Engineering, Hanyang University ERICA, Ansan, Gyeonggi-do 15588, South Korea (sj2527@hanyang.ac.kr)

*) Corresponding authors

Abstract – This paper presents an analytical model to describe the influence of mechanical deformation on the effective electrical conductivity of CNTs reinforced composites. The model shows that the effect of mechanical strain on the effective electrical conductivity of CNTs reinforced composites are via two mechanisms; one is the strain-induced alteration of volume fraction of inclusions and the other is the strain-induced change of the tunnelling electrical conductivity of inclusions. Analytical formulations are developed for calculating the dependence of the effective electrical conductivity of the composite on the mechanical strain. The model is validated by using experimental data published in literature for CNTs reinforced polymer composites.

Keywords: Carbon nanotubes; composites; electrical conductivity; strain; piezo-resistivity.

1. Introduction

Nanocomposite materials represent one of the fast-growing technologies in recent years. Carbon nanotubes (CNTs) have excellent thermal, electrical and mechanical properties [1]. CNTs have been incorporated into various materials to improve their performance [2,3] or make smart materials [4,5]. It is now well understood that in polymer composites filled with CNTs, their thermal and electrical conductivities change substantially with applied strains. The piezoresistive behaviour of the polymer composites with embedded CNTs forms the basis for using the composite itself as strain sensors for structural health monitoring [6,7].

In order to design and optimize the composite sensors, it is necessary to develop theoretical models capable of representing the relationship between their effective electrical conductivity (EEC) and the mechanical strain applied. In literature there have been numerous studies on the piezoresistive behaviours of polymer composites with embedded CNTs. For example, Böger et al. [8] experimentally investigated the electrical conductivity of epoxy resin filled with CNTs and carbon black. During the mechanical tests of the specimens the electrical conductivity of

the nanocomposite was also monitored and the relationship between the mechanical strain and electrical conductivity of the material was identified. Park et al. [9] studied the strain-dependent electrical resistance of multi-walled CNTs reinforced polyethylene oxide composites. It was shown that the electrical resistance of the composites increases initially linearly and then nonlinearly with the applied strain. Li and Chou [10] developed a two-dimensional finite element model to analyse the damage detecting mechanism in fibre composites using CNTs networks. Hu et al. [11] developed a three-dimensional numerical simulation model, in which the CNTs reorientation under the applied strain was simplified as rigid-body movement and was used to calculate the tunnelling resistance between the contacted CNTs and the overall piezoresistive properties of the composite. Kang et al. [12] investigated the effect of percolation threshold on the piezoresistive characteristics of CNTs/polyimide composites. Yasuoka et al. [13] reported their experimental results on the electrical resistance change of CNTs reinforced epoxy composites when subjected to applied strains. Alamusi et al. [14] presented a three-dimensional numerical model to simulate the piezoresistivity of CNT/polymer composites. Oliva-Aviles et al. [15] investigated the influence of CNTs alignment on the piezoresistivity of multi-walled CNTs/polymer composites. It was shown that the alignment of CNTs improved the strain sensing capability of the nanocomposites. Li et al. [16] developed an in-situ sensor using woven glass fabric reinforced epoxy composites filled with CNTs-Al₂O₃ hybrids to monitor the damage initiation and propagation under mechanical loading. The hybrids with CNTs grown on Al₂O₃ micro-spheres were synthesized by chemical vapor deposition. The electrical resistance of the composites was measured during quasi-static tensile tests. It was found that the electrical resistance response of the composites to the strain change could reflect various different damage modes of the composites, including microcracks, fibre/matrix interfacial debonding, transverse cracks, delamination, and fibre breakage. Konsta-Gdoutos and Aza [17] investigated the self-sensing properties of cementitious composites reinforced with well dispersed CNTs and carbon nanofibers. Their results demonstrated the piezoresistive properties of the nano-composites when they were under the action of cyclic compressive loading. Han et al. [18] studied the mechanical, electrically-conductive, and piezoresistive behaviours of smart cement mortars filled with CNTs and carbon nano-black. It was found that the CNTs and carbon nano-black fillers can effectively enhance the flexural strength and electrical conductivity of cement mortars and provide stable and sensitive piezoresistivity to the cement mortars at low filler contents. Pissis et al. [19] reported their work on the use of electrical DC measurement to monitor strain and to follow the onset and evolution of damage in composites made from poly-propylene filled with multi-walled CNTs, styrene butadiene rubber filled with carbon black, and poly-ether-ether-ketone reinforced with carbon fibres. Aviles et al. [20] examined the influence of CNTs on the piezoresistive behaviour of multi-walled CNTs/polymer composites. It was found that the electromechanical behaviour of CNTs reinforced composites is strongly influenced by the mechanical properties of the matrix and the aspect ratio of CNTs. García-Macías et al. [21] presented an electromechanical model of DC electrical resistance of CNTs reinforced cement paste sensors based on a piezoelectric lumped circuit. Deplancke et al. [22] investigated the impact of CNTs pre-localization on the ultra-low electrical percolation threshold and on the mechanical behaviour of sintered ultra-high molecular weight polyethylene based nanocomposites. García-Macías et al. [23] presented a mixed micromechanics and finite element approach for the analysis of CNTs-reinforced

composites subjected to arbitrary strain states. Two mechanisms that contribute to the electrical conductivity of CNTs-reinforced composites, namely the electron hopping and the conductive networking, are contemplated within a percolation framework in the micromechanics model. Alian and Meguid [24] developed a coupled electromechanical model for CNTs-reinforced composites, in which the representative volume element (RVE) of polymer matrix filled randomly with CNTs was generated using Monte-Carlo based algorithm. The model was used to compute the piezoresistive behaviour of CNTs-epoxy composites under tension, compression, and shear loads. The results showed that the composite gauge factor can reach up to 3.95 and is sensitive to the loading direction and CNTs volume fraction. Tanabi and Erdal [25] performed a series of experiments to examine the effects of dispersion process parameters and CNTs concentration on the electrical, mechanical and strain sensing properties of CNTs/epoxy nanocomposites. It was found that the nanocomposites fabricated by dispersing of lower amount of CNTs with high mixing speeds and long mixing times improved sensory properties and were more suitable for strain sensing applications. Sánchez-Romate et al. [26] proposed an analytical model for determining the electrical and electromechanical properties of CNTs nanocomposites. The model was developed based on the tunnelling mechanism of CNTs. Microscopy analysis and electrical and strain monitoring tests were also carried out on CNTs nanocomposites to demonstrate their model. Chen et al. [27] also developed a coupled electromechanical model for CNTs-reinforced composites. The model is similar to one given in literature [24], which used the Monte-Carlo based algorithm to generate the RVE of a two-phase composite (matrix and CNTs). The percolating CNTs networks were identified and transformed into an equivalent electric circuit consisting of tunnelling and intrinsic resistances. The electrical conductivity of the composite was obtained by using the modified nodal analysis method. After the structural analysis the displacements of the deformed CNTs were updated in the electrical model for calculating the corresponding tunnelling distances and the resistance of the deformed system. More recently, Jang and Li [28] presented an experimental investigation on the effects of thermal and mechanical loading on the effective electrical conductivity of carbon nanotube-polymer composites.

The above-described literature survey shows that there have been numerous experimental and numerical investigations on the piezoresistive properties of CNTs reinforced composites. However, very limited analytical work exists in literature to describe the piezoresistive behaviour of nanocomposites under the action of thermal and/or mechanical loadings. The aim of the present paper is to develop an analytical model which is able to describe the effect of the externally applied mechanical strain on the electrical conductivity of CNTs reinforced composites. Analytical formulations for calculating the electrical conductivity of the composites are derived based on the strain-induced changes in the volume fraction and tunnelling conductivity of inclusions. To demonstrate the present model, comparisons between the present analytical solution and existing experimental result are also provided for a number of different loading cases.

2. Calculation of electrical conductivity of two-component constituted composites

Recently, Fang et al. [29] proposed a simple analytical model for calculating the electrical conductivity of composites constituted with two components, named the inclusions and medium (or matrix). The model was developed based on the conventional spherical model by considering the effect of aspect ratio of inclusions, in which the EEC of the composite is expressed as follows,

$$\sigma_e = \frac{2V_m\sigma_m^2 + (3V_i + V_m)\sigma_i\sigma_m}{(3V_i + 2V_m)\sigma_m + V_m\sigma_i} [1 - f(V_i)] + \frac{2V_i\sigma_i^2 + (3V_m + V_i)\sigma_i\sigma_m}{(3V_m + 2V_i)\sigma_i + V_i\sigma_m} f(V_i) \quad (1)$$

where σ_e is the EEC of the composite, σ_i and V_i are the electrical conductivity and volume fraction of the inclusions, σ_m and V_m are the electrical conductivity and volume fraction of the medium, respectively, $f(V_i)$ is the weight function, which is defined as follows,

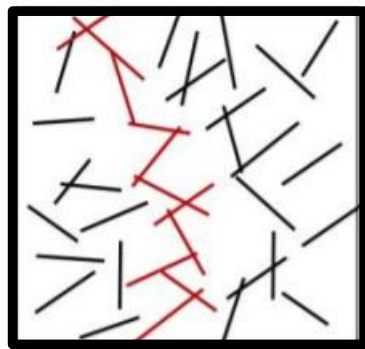
$$f(V_i) = \begin{cases} 0 & V_i \leq V_{i,th} \\ \left(\frac{V_i - V_{i,th}}{1 - V_{i,th}}\right)^\alpha & V_i > V_{i,th} \end{cases} \quad (2)$$

where α is a constant, $V_{i,th} = 3/\lambda^2 - 2/\lambda^3$ is the percolation threshold of the composite or the threshold volume fraction of the inclusions, and λ is the aspect ratio of inclusions. For the composite in which the inclusions and medium have distinct electrical properties, that is $\sigma_i \gg \sigma_m$, Eq.(1) can be simplified as follows,

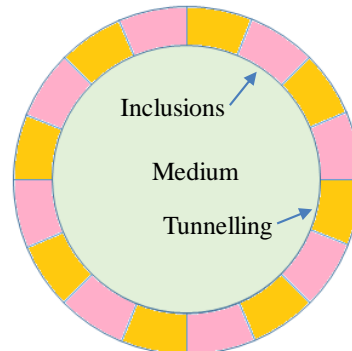
$$\sigma_e = \begin{cases} 0 & V_i \leq V_{i,th} \\ \frac{2V_i\sigma_i}{3 - V_i} \left(\frac{V_i - V_{i,th}}{1 - V_{i,th}}\right)^\alpha & V_i > V_{i,th} \end{cases} \quad (3)$$

Eq.(3) indicates that the EEC of the composite with strongly distinct electrical properties in its two constituted components is mainly dependent on the electrical conductivity and volume fraction of the inclusions, and the percolation threshold of the composite. If the volume fraction of the inclusions is not greater than its threshold value, the EEC of the composite can be ignored.

Note that Eq.(3) was developed based on the assumption of perfect connections between inclusions. When the tunnelling between inclusions in the composite is considered a reduced electrical conductivity for the inclusions should be utilised.



(a)



(b)

Fig.1 (a) RVE of CNTs reinforced polymer composite (connective (red) and non-connective (black) inclusions). (b) Spherical model of two-component composite with considering tunnelling effect of inclusions.

Assume that the inclusions are connected in series in the spherical model and the conductivity at connections is represented by the representative tunnelling electrical conductivity (see Fig.1). In this case, the EEC of the inclusions in the spherical model can be calculated as follows,

$$\sigma_i = \frac{\sigma_{io}\sigma_{it}}{\beta\sigma_{io}+(1-\beta)\sigma_{it}} \quad (4)$$

where σ_i is the EEC of the inclusions in the spherical model with considering their tunnelling effect, σ_{io} is the electrical conductivity of the inclusion material, σ_{it} is the tunnelling electrical conductivity of the inclusions, and $1 \geq \beta \geq 0$ is a constant representing the contribution of tunnelling. Substituting Eq.(4) into (3), for $V_i > V_{i,th}$, it yields,

$$\sigma_e = \frac{2V_i\sigma_{io}}{3-V_i} \left(\frac{V_i-V_{i,th}}{1-V_{i,th}} \right)^\alpha \frac{\sigma_{it}}{\beta\sigma_{io}+(1-\beta)\sigma_{it}} \quad (5)$$

When Eq.(5) is applied to the CNTs reinforced composites, according to the Landauer-Buttiker formula [30], the tunnelling electrical conductivity of inclusions can be approximated as follows,

$$\sigma_{it} = \frac{2e^2}{h} MJ \quad (6)$$

where e is the electron charge, h is the Planck's constant, M is the total number of conduction channels, and J is the transmission probability of an electron through the matrix barrier between two CNTs, which can be obtained by solving the Schrödinger equation or obtained from the WKB approximation [31,32,33],

$$J = \begin{cases} \exp\left(-\frac{d_{vdW}}{d_{tunnel}}\right) & 0 \leq d - D \leq d_{vdW} \\ \exp\left(-\frac{d-D}{d_{tunnel}}\right) & d_{vdW} \leq d - D \leq d_{cutoff} \end{cases} \quad (7)$$

where d is the minimum distance between the axes of two neighbouring CNTs where electron tunnelling is most likely to occur, d_{vdW} and d_{cutoff} are the distances representing the lower-bound and upper-bound of the distance d , respectively, d_{tunnel} is the constant representing the tunnelling characteristic length, and D is the diameter of the CNTs. If d is greater than the distance of $D+d_{cutoff}$ then the tunnelling electrical resistance becomes infinite and thus $J=0$. If d is shorter than the distance of $D+d_{vdW}$ then the tunnelling electrical resistance reaches to its lowest value and thus J becomes constant. Eq.(7) indicates that the transmission probability J decreases in an exponential function of the distance between two neighbouring CNTs.

3. Effect of mechanical loading on electrical conductivity of CNTs reinforced composites

In order to consider the effect of externally applied mechanical loading on the EEC of CNTs reinforced composites, we consider a unit volume of the RVE of the composite. After it is

subjected to a mechanical loading in x-direction, the volume of the RVE changes. The new volume of the RVE can be expressed as follows,

$$V_{c,new} = (1 + \varepsilon_x)(1 - \nu_c \varepsilon_x)(1 - \nu_c \varepsilon_x) \quad (8)$$

where $V_{c,new}$ is the new volume of the deformed composite, ε_x is the normal strain of the composite in x-direction, and ν_c is the Poisson's ratio of the composite. The volume increase in the composite is attributed to the volume increases in both the medium and inclusions. For most of CNTs reinforced composites, they have the following features: (1) the volume fraction of CNTs in the composite is much lower than that of the medium; (2) the stiffness of CNTs is much greater than that of the medium material; (3) the CNTs used in the composite normally have large aspect ratio. Assuming that the CNTs are equally dispersed in x-, y- and z-axial directions, the new volume of CNTs in the RVE caused by the strain ε_x of the composite can be approximately expressed as,

$$V_{i,new} = \left(1 + \frac{1-2\nu_i}{3} \varepsilon_x\right) V_i \quad (9)$$

where $V_{i,new}$ is the volume of CNTs in the deformed composite and ν_i is the Poisson's ratio of the CNTs. By using the assumption of small strains, the new volume fraction of the CNTs in the deformed composite, V_i^* , thus can be expressed as follows,

$$V_i^* = \frac{V_{i,new}}{V_{c,new}} = \frac{1 + \frac{1-2\nu_i}{3} \varepsilon_x}{(1 + \varepsilon_x)(1 - \nu_c \varepsilon_x)(1 - \nu_c \varepsilon_x)} V_i \approx \left[1 - \frac{2}{3}(1 + \nu_i - 3\nu_c) \varepsilon_x\right] V_i \quad (10)$$

Note that the strain ε_x of the composite not only causes the change of volume fraction of CNTs in the composite, but also leads to the change of the tunnelling probability and thus the alteration of the tunnelling electrical conductivity. Assume that the new minimum distance between the axes of two neighbouring CNTs in the deformed composite is expressed as $(d-D)(1+\varepsilon_x)+D$. According Eqs.(6) and (7), the new tunnelling electrical conductivity of the CNTs in the deformed composite can be expressed as follows,

$$\sigma_{it}^* \approx \sigma_{it}(1 - \gamma \varepsilon_x) \quad (11)$$

where σ_{it}^* is the new tunnelling electrical conductivity of the CNTs in the deformed composite, and $\gamma=(d-D)/d_{\text{tunnel}}$ is a dimensionless parameter. Note that Eq.(11) is applicable only when $d_{\text{vdW}} < (d-D)(1+\varepsilon_x)+D < d_{\text{cutoff}}$. If $(d-D)(1+\varepsilon_x)+D < d_{\text{vdW}}$, $\sigma_{it}^* = \sigma_{it}$; and if $(d-D)(1+\varepsilon_x)+D > d_{\text{cutoff}}$, $\sigma_{it}^* = 0$. The latter represents the case where the percolation of the composite is broken. Also, it should be noted that Eq.(11) is only for a representative tunnelling distance. When it is applied to the RVE, a correction coefficient need be introduced by considering the fact that the REV involves many parallel or series connected tunnelling distances. Thus, Eq.(11) is modified as follows,

$$\sigma_{it}^* = \sigma_{it}(1 - \mu \gamma \varepsilon_x) \quad (12)$$

where μ is a dimensionless constant representing the effect of the group tunnelling distances in RVE on the calculation of the representative tunnelling electrical conductivity of the CNTs. Additionally, since both σ_{it}^* and ε_x are the direction-dependent parameters, the value of γ for the case where σ_{it}^* and ε_x are in the same direction would be different from that for the case where σ_{it}^* and ε_x are in different directions.

Substituting V_i and σ_{it} in Eq.(5) with V_i^* defined by Eq.(10) and σ_{it}^* defined by Eq.(12), it yields,

$$\sigma_e^* = \frac{2\left[1-\frac{2}{3}(1+v_i-3v_c)\varepsilon_x\right]V_i\sigma_{io}}{3-\left[1-\frac{2}{3}(1+v_i-3v_c)\varepsilon_x\right]V_i} \left(\frac{\left[1-\frac{2}{3}(1+v_i-3v_c)\varepsilon_x\right]V_i-V_{i,th}}{1-V_{i,th}}\right)^\alpha \frac{\sigma_{it}(1-\mu\gamma\varepsilon_x)}{\beta\sigma_{io}+(1-\beta)\sigma_{it}(1-\mu\gamma\varepsilon_x)} \quad (13)$$

where σ_e^* is the new EEC of the deformed composite. The relative change of the EEC of the composite caused by the strain ε_x thus can be expressed as follows,

$$\frac{\Delta\sigma_e}{\sigma_e} = \frac{\sigma_e^* - \sigma_e}{\sigma_e} = \frac{\sigma_e^*}{\sigma_e} - 1 \quad (14)$$

where σ_e^* and σ_e are calculated using Eq.(13) and Eq.(5), respectively. Eq.(13) shows that the influence of the mechanical strain on the EEC of the composite can be evaluated by two parts. One is its influence on the volume fraction of inclusions; the other is its influence on the tunnelling conductivity. **Figs.2 and 3** graphically show the individual influences of the mechanical strain on the EEC of the CNTs reinforced composite via the volume fraction of inclusions and the tunnelling conductivity. The parameters employed in the calculation are: $\sigma_{io}=1.0 \times 10^4$ S/m (for MWCNTs), $\sigma_{it}=250$ S/m (for CNTs tunnelling), $V_{i,th}=0.326\%$ (for CNTs' aspect ratio of 30), $v_c=0.30$, $v_i=0.17$, $\alpha=1.0$, $\beta=0.20$, $\mu=1.0$, $\gamma=0.20$ (when $V_i=2\%$) and $\gamma=0.40$ (when $V_i=0.5\%$) [27].

The results shown in **Fig.2** consider only the influence of volume fraction change of inclusions caused by the strain while the tunnelling conductivity change is ignored (that is $\sigma_{it}^* \equiv \sigma_{it}$). It can be seen from the figure that the relative change of EEC of the composite is nearly linear with the strain. This indicates that for small strains linear relationships hold between the strain, the volume fraction change of inclusions, and the EEC change of the composite. The linear relationship is also demonstrated by the fact that the changes of the EEC of the composite to the tensile and compressive strains are almost identical but with opposite signs. The compression of the composite leads an increase of the EEC; whereas the tension of the composite leads a decrease of the EEC. It is also observed from the figure that the relative change of the EEC of the composite is more significant in the composite with lower volume fraction of inclusions. This indicates that the composite with low volume fraction of inclusion is more sensitive to the strain. These features appear to be consistent with what were observed in the experiments [8,19] and numerical simulations [24,27].

The results shown in **Fig.3** consider only the influence of tunnelling conductivity change caused by the strain while the volume fraction change of the inclusions is ignored (that is $V_i^* \equiv V_i$). It can be observed from the figure that the variation of the EEC of the composite is also nearly linear with the strain. The compression or tension of the composite leads to an increase or a decrease of the EEC of the composite. The influence of the strain-induced tunnelling conductivity change on the EEC of the composite is more significant on the composite with lower volume fraction of inclusions. It should be mentioned here that the dimensionless parameter γ depends on the volume fraction of inclusions. For the case where the volume fraction of inclusions is sufficiently large the distance between any two neighbouring CNTs would be smaller than d_{vdw} and thus in this case the strain will have no influence on the tunnelling conductivity. On the other hand, for the case where the volume fraction of inclusions is sufficiently small the distance between any two neighbouring CNTs would be larger than d_{cutoff} and thus in this case the tunnelling conductivity would be zero. **Fig.4**

shows the combined influence of the mechanical strain on the EEC of the CNTs reinforced composite via the volume fraction of inclusions and the tunnelling conductivity, in which the results plotted represent the sum of those shown in Fig.2 and Fig.3.

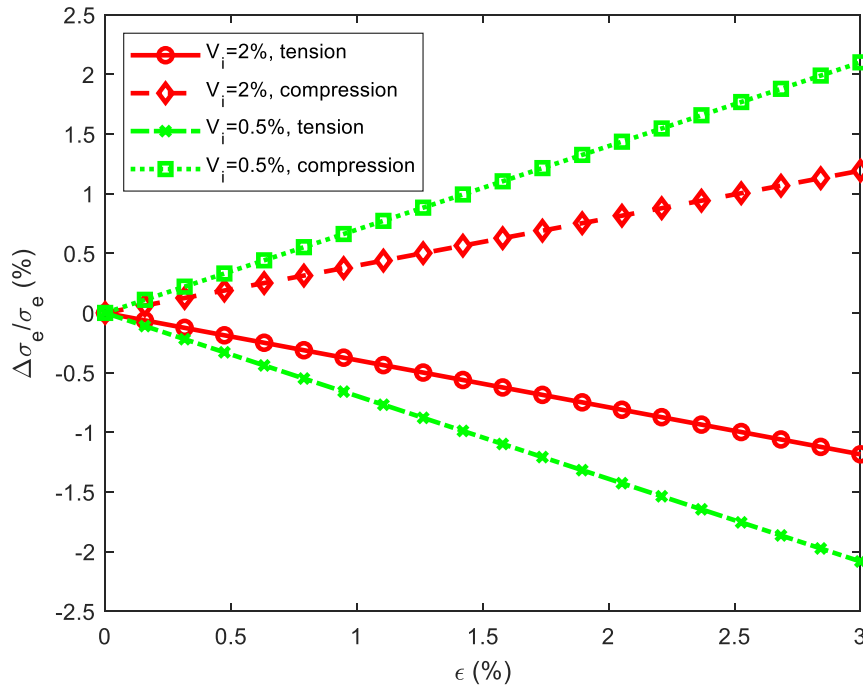


Fig.2 Variation of effective electrical conductivity of composite with axial tensile or compressive strain caused by volume fraction change of inclusions.

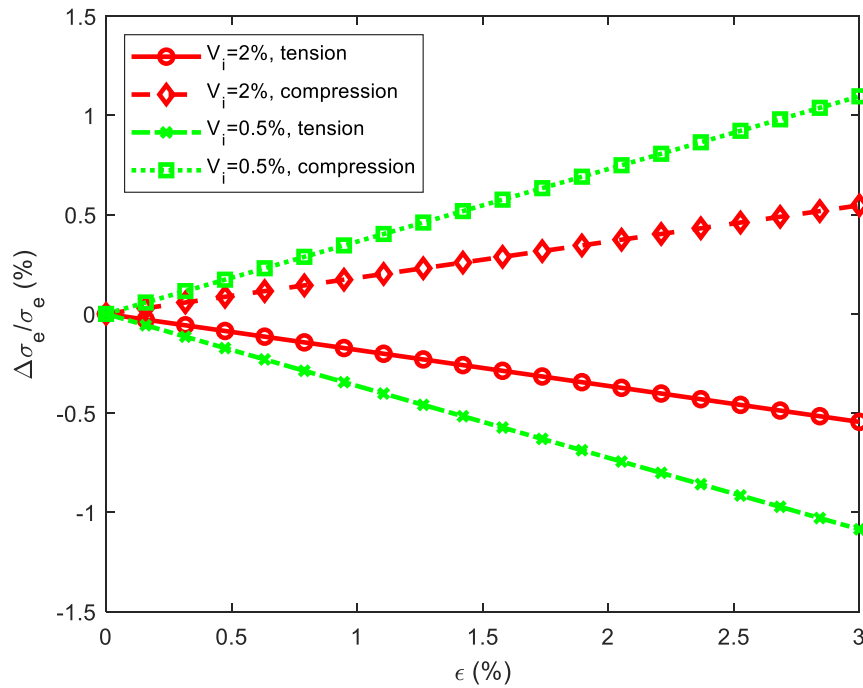


Fig.3 Variation of effective electrical conductivity of composite with axial tensile or compressive strain caused by tunnelling conductivity change.

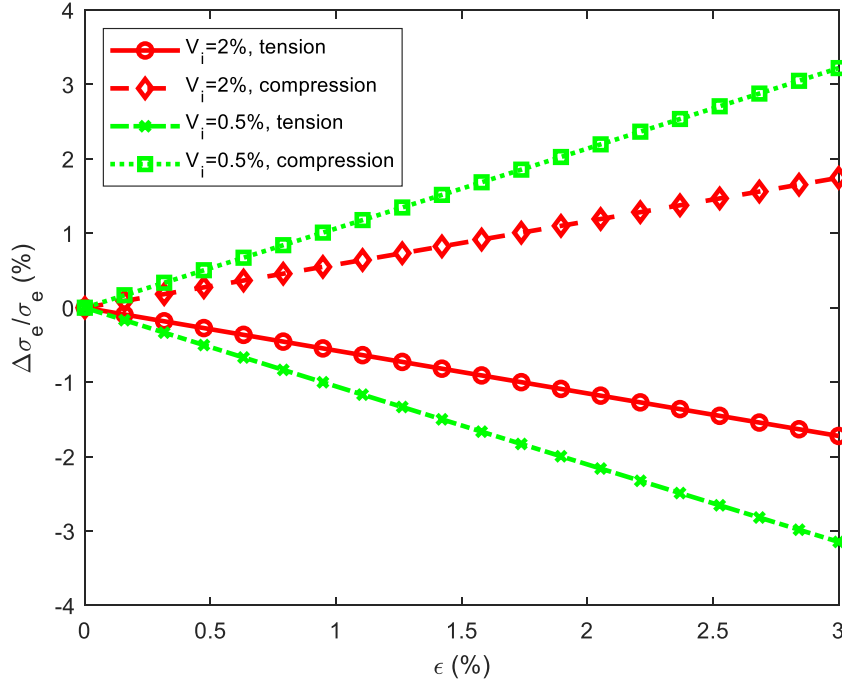


Fig.4 Variation of effective electrical conductivity of composite with axial tensile or compressive strain caused by both volume fraction change of inclusions and tunnelling conductivity change.

The analysis described above indicates that the change of the EEC of composites with axial tensile or compressive strain can be expressed in terms of its increment form. Note that for most CNTs reinforced composites the volume fraction of CNTs in the composites is very small, that is $V_i \ll 1$. In this case, Eq.(5) can be simplified as follows,

$$\sigma_e = \frac{2V_i\sigma_{io}}{3}(V_i - V_{i,th})^\alpha \frac{\sigma_{it}}{\beta\sigma_{io} + (1-\beta)\sigma_{it}} \quad (15)$$

By differentiating σ_e in Eq.(15) with respect to V_i and σ_{it} , respectively, it yields,

$$\Delta\sigma_e = \frac{(1+\alpha)V_i - V_{i,th}}{V_i(V_i - V_{i,th})} \sigma_e \Delta V_i + \frac{\beta\sigma_{io}}{\sigma_{it}[\beta\sigma_{io} + (1-\beta)\sigma_{it}]} \sigma_e \Delta\sigma_{it} \quad (16)$$

According to Eqs.(10) and (12), ΔV_i and $\Delta\sigma_{it}$ can be expressed in terms of the strain ϵ_x . Thus, Eq.(16) can be rewritten as,

$$\frac{\Delta\sigma_e}{\sigma_e} = - \left(\frac{2(1+\nu_i - 3\nu_c)[(1+\alpha)V_i - V_{i,th}]}{3(V_i - V_{i,th})} + \frac{\beta\mu\gamma\sigma_{io}}{\beta\sigma_{io} + (1-\beta)\sigma_{it}} \right) \epsilon_x \quad (17)$$

For most CNTs reinforced composites, we have $\sigma_{it} \ll \sigma_{io}$ and thus the second term inside the parentheses in the right hand side of Eq.(17) can be approximately taken as $\mu\gamma$. That is,

$$\frac{\Delta\sigma_e}{\sigma_e} = - \left(\frac{2(1+\nu_i - 3\nu_c)[(1+\alpha)V_i - V_{i,th}]}{3(V_i - V_{i,th})} + \mu\gamma \right) \epsilon_x \quad (18)$$

Fig.5 graphically shows the variation of the change rate of the relative EEC of CNTs reinforced composite with the volume fraction of inclusions at four different γ values, calculated from Eq.(18). It can be seen from the figure that the rate of change increases with increased γ value but decreases with increased volume fraction of inclusions. However, when the volume fraction of inclusions is much greater than its threshold value, the rate of change becomes insensitive to the volume fraction of inclusions, indicating that the influence of the volume fraction change of inclusion on $\Delta\sigma_e/\sigma_e$ becomes stabilized.

Physically, γ should be proportional to $V_{i,th}/V_i$. By assuming $\mu\gamma = k \left(\frac{V_{i,th}}{V_i}\right)^s$, Eq.(18) becomes,

$$\frac{\Delta\sigma_e}{\sigma_e} = - \left[\frac{2(1+\nu_i-3\nu_c)[(1+\alpha)V_i-V_{i,th}]}{3(V_i-V_{i,th})} + k \left(\frac{V_{i,th}}{V_i}\right)^s \right] \varepsilon_x \quad (19)$$

where s and k are the constants that can be determined by experimental data. Eq.(19) gives the prediction of the relative change of the EEC of CNTs reinforced composites with strain. The first and second terms in the parentheses reflect the influences of the strain-induced volume fraction change of CNTs and the strain-induced tunnelling conductivity change of CNTs in the composite, respectively. Physically, the parameter k reflects the weight of the tunnelling conductivity of CNTs on the EEC of the composite. The larger the k value, the more important of the tunnelling conductivity of CNTs on the EEC of the composite.

In most experiments, one usually measures the electrical resistance of the material. According to the reciprocal relation between the electrical resistance and electrical conductivity, the change in the electrical resistance of a composite due to the mechanical deformation can be expressed as follows,

$$\frac{\Delta R}{R} = \frac{R_{new}-R}{R} = \frac{R_{new}}{R} - 1 = \frac{\sigma_e}{\sigma_e+\Delta\sigma_e} - 1 = - \frac{\Delta\sigma_e}{\sigma_e} \quad (20)$$

where R and R_{new} are the electrical resistances of the undeformed and deformed composites, respectively, and ΔR is the corresponding change of the electrical resistance of the composite caused by mechanical deformation.

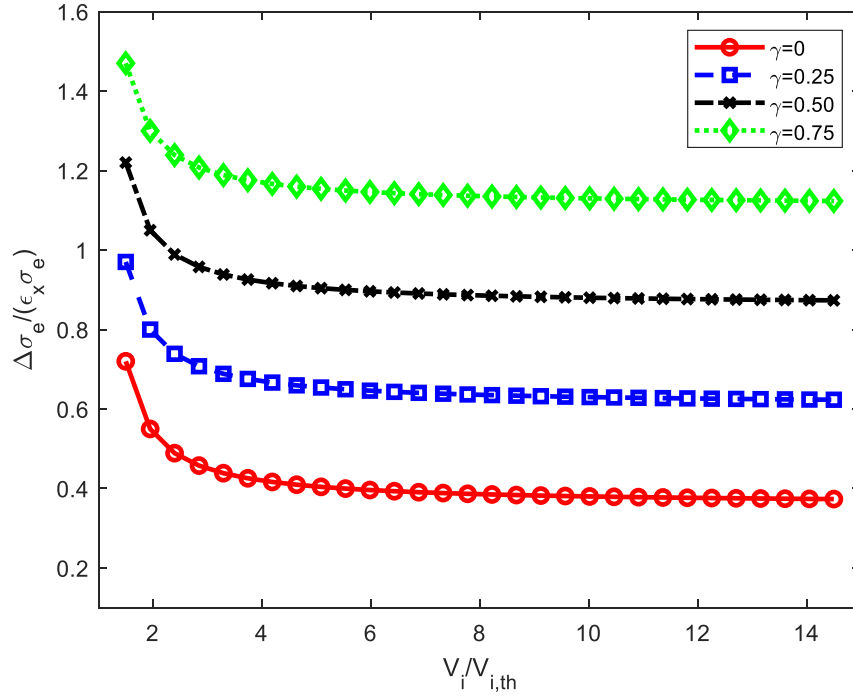


Fig.5 Change rate of relative effective electrical conductivity of composite with volume fraction of inclusions ($v_c=0.30$, $v_i=0.17$, $\mu=1.0$, $\alpha=1.0$).

4. Experimental validation of the model

To demonstrate the formulations developed in the preceding section, that is Eqs.(19) and (20), the comparisons between the calculated electrical resistance using Eqs.(19) and (20) and that measured in experiments are made for three different CNTs reinforced composites. The first one is the multi-walled CNTs reinforced polyethylene oxide composite films. The experimental data are the averages obtained from two repeat tensile tests of the specimens on which the multi-walled CNTs reinforced composite films were bonded [9]. The experiments used two representative volume fractions ($V_i=0.56\%$ and $V_i=1.44\%$) of multi-walled CNTs in composite films. In the calculations the Poisson's ratio is taken as $v_c=0.3$ for the composite and $v_i=0.17$ for the multi-walled CNTs, the percolation threshold is taken as $V_{i,th}=0.28\%$ which was commented in the experiments [9]. The other parameters used in calculations are $\alpha=1$ and $s=1/3$. Fig. 6 shows the best fit of the calculated electrical resistance with the experimentally measured data, which gives the fitting constant $k=25$. It is evident from the figure that there is a good agreement between the calculated and measured electrical resistances for the composites with two different CNTs volume fractions. A large k value reflects the sensitivity of the EEC of the composite to the tunnelling conductivity of the CNTs. This is probably due to the two-dimensional nature of the composites used in the tests.

The second set of experimental data were obtained from the compressive tests of carbon-fibres reinforced epoxy composites [13,27]. The composites tested used two volume fractions ($V_i=0.50\%$ and $V_i=2.0\%$) of carbon-fibres. The percolation threshold of inclusions in the composites is about $V_{i,th}=0.35\%$. Similar to Fig.6, in the calculations the Poisson's ratio is taken

as $v_c=0.3$ for the composite and $v_i=0.17$ for the carbon-fibres, the two other parameters are also taken as $\alpha=1$ and $s=1/3$. Fig. 7 shows the best fit of the calculated electrical resistance with the experimentally measured data, which gives the fitting constant $k=0$. This means that for the carbon-fibres reinforced epoxy composites the change of EEC of the composites is mainly caused by the volume fraction change of carbon-fibres in the composites. This is probably due to the fact that the carbon-fibres used in the experiments are well dispersed, which makes the tunnelling conductivity less sensitive to the deformation. Again, it is observed from the figure that the prediction is in good agreement with the experimental data for the composites with two different volume fractions of inclusions.

The third set of experimental data were obtained from the tensile tests of CNTs-reinforced epoxy composites [34]. The experiments used two mass fractions of CNTs (0.2% and 0.5%). According to the following relationship between the volume fraction V_i and mass fractions m_i of CNTs in the composite,

$$V_i = \frac{m_i \rho_m}{m_i \rho_m + (1 - m_i) \rho_i} \quad (21)$$

where $\rho_i=2250 \text{ kg/m}^3$ and $\rho_m=1150 \text{ kg/m}^3$ are the densities of the CNTs and hardened epoxy resin, respectively, their corresponding volume fractions are $V_i=0.102\%$ and $V_i=0.256\%$. Fig. 8 shows the comparison between the calculated and measured electrical resistances of the CNTs-reinforced composites. Again, the test data are the averages obtained from two repeat tests. In the calculations the Poisson's ratio is taken as $v_c=0.3$ for the composite and $v_i=0.17$ for the CNTs, the two other parameters are also taken as $\alpha=1$ and $s=1/3$. The percolation threshold of CNTs in the composites is taken as $V_{i,th}=0.077\%$ because of the large aspect ratio of CNTs employed. The fitting constant is found to be $k=1.64$. It can be seen from the figure that the predicted electrical resistance is in very good agreement with the experimental data. This demonstrates that the present model is appropriate although mathematically it is very simple.

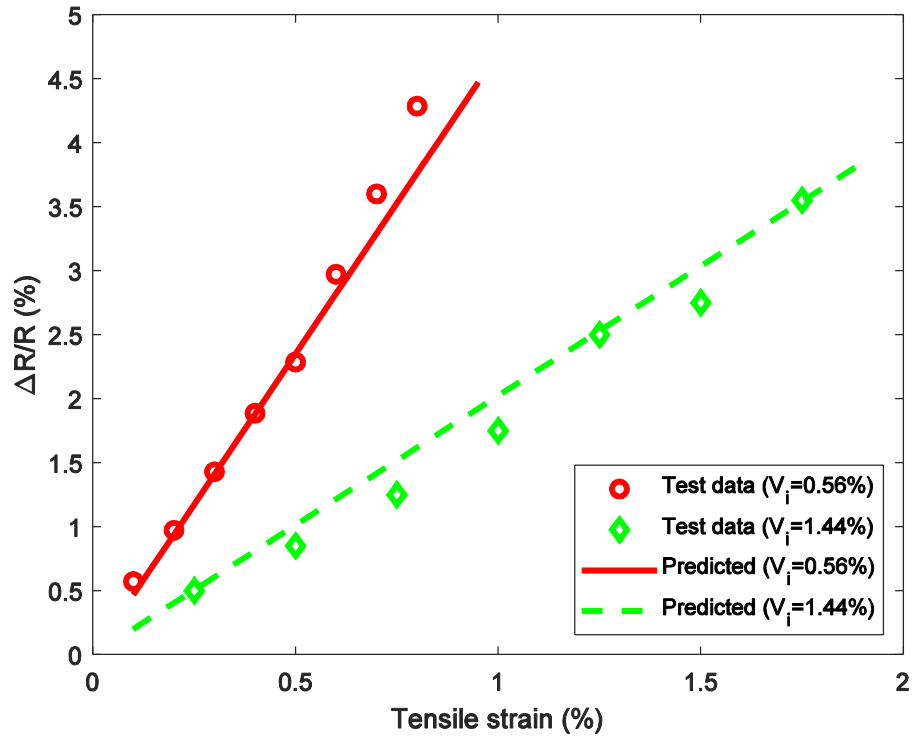


Fig.6 Comparison of calculated and measured electrical resistances of multi-walled CNTs/polymer composite films ($v_c=0.3$, $v_i=0.17$, $\alpha=1$, $s=1/3$, $k=25$, $V_{i,th}=0.28\%$).

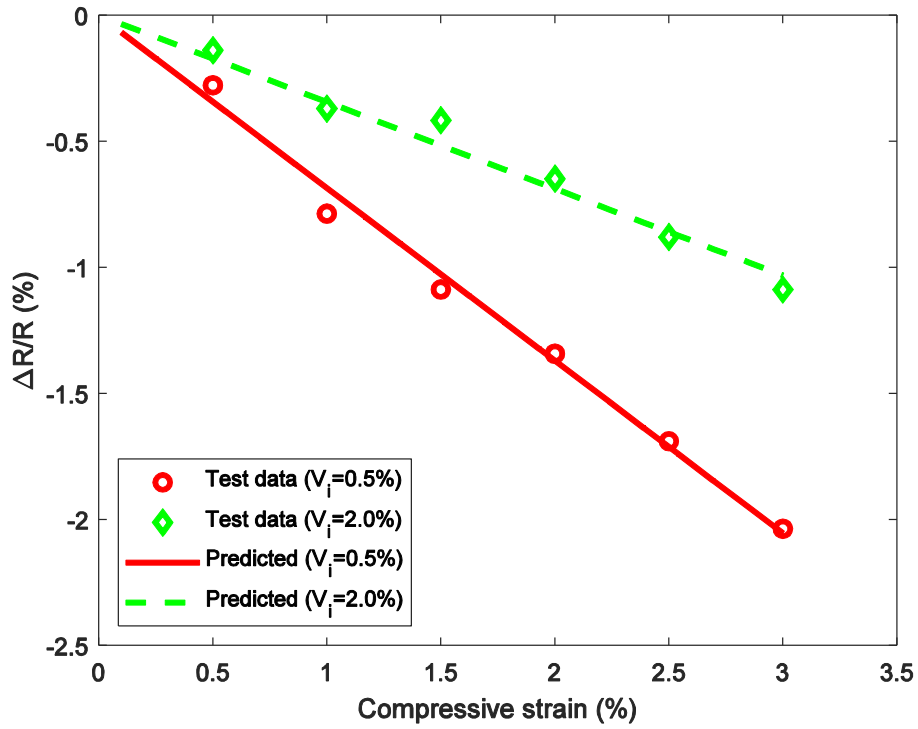


Fig.7 Comparison of calculated and measured electrical resistances of CNFs/epoxy nanocomposites ($v_c=0.3$, $v_i=0.17$, $\alpha=1$, $s=1/3$, $k=0$, $V_{i,th}=0.35\%$).

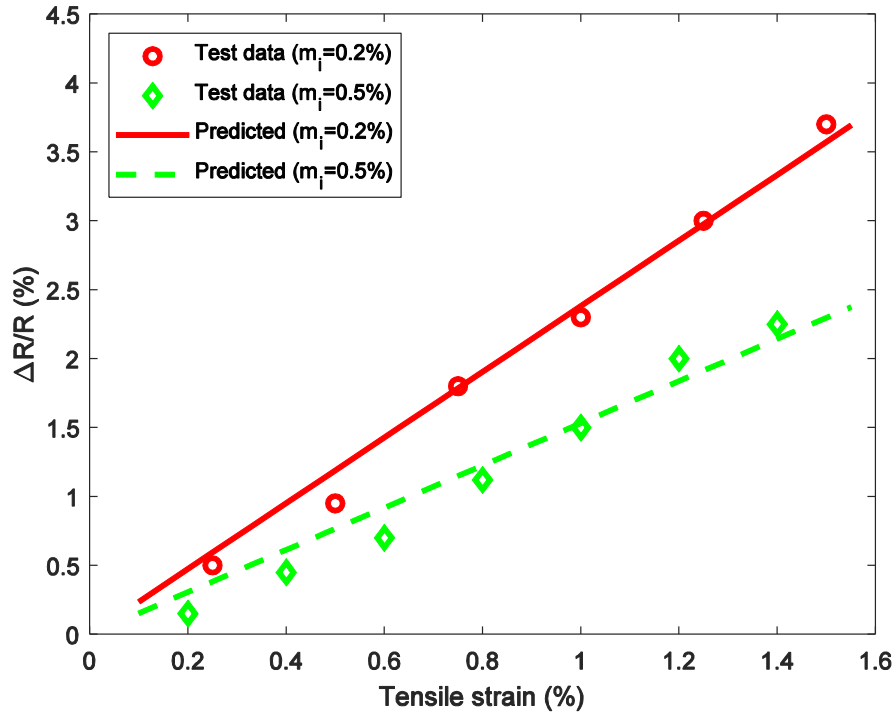


Fig.8 Comparison of calculated and measured electrical resistances of CNTs/epoxy nanocomposites ($v_c=0.3$, $v_i=0.17$, $\alpha=1$, $s=1/3$, $k=1.64$, $V_{i,th}=0.077\%$).

5. Conclusions

This paper has presented an analytical study on the influence of the mechanical strain on the EEC of CNTs reinforced composites. Analytical formulations have been derived for calculating the dependence of the EEC of the composite on the mechanical strain. The analytical model has been validated by using experimental data published in literature for CNTs reinforced polymer composites. From the present study the following conclusions can be drawn.

- The influence of mechanical strain on the EEC of CNTs reinforced composites can be apportioned by considering its individual influences on the volume fraction change of inclusions and the tunnelling conductivity change of CNTs in the composites. The influence functions of the volume fraction of inclusions and the tunnelling conductivity on the EEC of the composites have been derived.
- Under the assumption of small strains, both the strain-induced volume fraction change of inclusions and the strain-induced tunnelling conductivity change of CNTs can be treated as the linear functions of the strain. The relative change of the EEC of the CNTs reinforced composites resulted from the strain-induced volume fraction change of

inclusions or the strain-induced tunnelling conductivity change of CNTs is also found to be almost linear with the strain.

- The influence of the mechanical strain on the EEC of the CNTs reinforced composites is found to depend on the volume fraction of inclusions and the tunnelling distance between two neighbouring CNTs. The mechanical strain has more influence on the EEC of the composite with lower volume fraction of inclusions or longer tunnelling distance than that with higher volume fraction of inclusions or shorter tunnelling distance.
- The compressive strain leads to an increase of the EEC of the CNTs reinforced composites; whereas the tensile strain leads to a decrease of the EEC of the CNTs reinforced composites. However, the increase rates or decrease rates of the EEC of the CNTs reinforced composites are different in different directions. The EEC change resulted from the strain-induced volume fraction change of inclusions has no directionality; but the EEC change resulted from the strain-induced tunnelling conductivity change has. Thus, the directions of conductivity and mechanical strain used in calculations or experiments should be indicated.

Acknowledgments – The work presented in the paper was supported by the Korean Agency for Infrastructure Technology Advancement (KAIA) via a grant funded to the University of Plymouth by the Ministry of Land, Infrastructure and Transport (19CTAP-C151808-01), South Korea and the UK Royal Academy of Engineering via the Frontiers of Development Programme (FoDSF\1920\2\100007).

Declaration of interests - The authors declare that they have no known competing financial interests or personal relationships that could have appeared to influence the work reported in this paper.

References

- [1] M. Paradise, T. Goswami, Carbon nanotubes – production and industrial applications. *Materials & Design* 28(5) (2007) 1477-1489.
- [2] N. Muralidharan, E. Teblum, A.S. Westover, D. Schauben, A. Itzhak, M. Muallem, G.D. Nessim, C.L. Pint, Carbon nanotube reinforced structural composite supercapacitor. *Scientific Reports* 8 (2018) 17662 (<https://doi.org/10.1038/s41598-018-34963-x>).
- [3] S.R. Bakshi, D. Lahiri, A. Agarwal, Carbon nanotube reinforced metal matrix composites - a review. *International Materials Reviews* 55(1) (2010), 41-64,
- [4] I. Kang, Y.Y. Heung, J.H. Kim, J.W. Lee, R. Gollapudi, S. Subramaniam, S. Narasimhadevara, D. Hurd, G.R. Kirikera, V. Shanov, M.J. Schulz, D. Shi, J. Boerio, S. Mall, M. Ruggles-Wren, Introduction to carbon nanotube and nanofiber smart materials. *Composites Part B: Engineering* 37 (6) (2006) 382-394.
- [5] B.R.C. de Menezes, K.F. Rodrigues, B.C. da Silva Fonseca, R.G. Ribas, T.L. do Amaral Montanheiro, G.P. Thim, Recent advances in the use of carbon nanotubes as smart biomaterials. *J. Mater. Chem. B* 7 (2019) 1343-1360.

- [6] C. Li, E.T. Thostenson, T.W. Chou, Sensors and actuators based on carbon nanotubes and their composites: a review. *Composites Science and Technology* 68(6) (2008) 1227–1249.
- [7] N. Hu, H. Fukunaga, S. Atobe, Y. Liu, J. Li, Piezoresistive strain sensors made from carbon nanotubes based polymer nanocomposites. *Sensors* 11(11) (2011) 10691–10723.
- [8] L. Böger, M.H.G. Wichmann, L.O. Meyer, K. Schulte, Load and health monitoring in glass fibre reinforced composites with an electrically conductive nanocomposite epoxy matrix. *Composites Science and Technology* 68(7/8) (2008) 1886–1894.
- [9] M. Park, H. Kim, J.P. Youngblood, Strain-dependent electrical resistance of multi-walled carbon nanotube/polymer composite films. *Nanotechnology* 19(5) (2008) 055705.
- [10] C. Li, T.W. Chou, Modelling of damage sensing in fibre composites using carbon nanotube networks. *Compos. Sci. Technol.* 68(15/16) (2008) 3373–3379.
- [11] N. Hu, Y. Karube, C. Yan, Z. Masuda, H. Fukunaga, Tunneling effect in a polymer/carbon nanotube nanocomposite strain sensor. *Acta Mater.* 56(13) (2008), 2929–2936.
- [12] J.H. Kang, C. Park, J.A. Scholl, A.H., Brazin, N.M. Holloway, J.W. High, S.E. Lowther, J.S. Harrison, Piezoresistive characteristics of single wall carbon nanotube/polyimide nanocomposites. *J. Polym. Sci., Part B: Polym. Phys.* 47(10) (2009) 994–1003.
- [13] T. Yasuoka, Y. Shimamura, A. Todoroki, Electrical resistance change under strain of CNF/flexible-epoxy composite. *Adv. Compos. Mater.* 19(2) (2010) 123–138.
- [14] Alamusi, Y.L. Liu, N. Hu, Numerical simulations on piezoresistivity of CNT/polymer based nanocomposites. *CMC-Computers, Materials & Continua* 20(2) (2010) 101–117.
- [15] A.I. Oliva-Aviles, F. Aviles, V. Sosa, Electrical and piezoresistive properties of multi-walled carbon nanotube/polymer composite films aligned by an electric field. *Carbon* 49(9) (2011), 2989–2997.
- [16] W. Li, D. He, Z. Dang, J. Bai, In situ damage sensing in the glass fabric reinforced epoxy composites containing CNT–Al₂O₃ hybrids. *Composites Science and Technology* 99 (2014) 8–14.
- [17] M.S. Konsta-Gdoutos, C.A. Aza, Self sensing carbon nanotube (CNT) and nanofiber (CNF) cementitious composites for real time damage assessment in smart structures. *Cement and Concrete Composites* 53 (2014) 162–169.
- [18] B. Han, L. Zhang, S. Sun, X. Yu, X. Dong, T. Wu, J. Ou, Electrostatic self-assembled carbon nanotube/nano carbon black composite fillers reinforced cement-based materials with multifunctionality. *Composites Part A: Applied Science and Manufacturing* 79 (2015) 103–115.
- [19] P. Pissis, G. Georgousis, C. Pandis, P. Georgiopoulos, A. Kyritsis, E. Kontou, M. Micusik, K. Czanikova, M. Omastova, Strain and damage sensing in polymer composites and nanocomposites with conducting fillers. *Procedia Engineering* 114 (2015) 590–597.
- [20] F. Aviles, A. May-Pat, G. Canche-Escamilla, O. Rodríguez-Uicab, J.J. Ku-Herrera, S. Duarte-Aranda, J. Uribe-Calderon, P.I. Gonzalez-Chi, L. Arronche, V. La Saponara, Influence of carbon nanotube on the piezoresistive behaviour of multiwall carbon nanotube/polymer composites. *J. Intell. Mater. Syst. Struct.* 27(1) (2016) 92–103.
- [21] E. García-Macías, A. Downey, A. D'Alessandro, R. Castro-Triguero, S. Laflamme, F. Ubertini, Enhanced lumped circuit model for smart nanocomposite cement-based sensors under dynamic compressive loading conditions. *Sensors and Actuators A: Physical* 260 (2017) 45–57.

- [22] T. Deplancke, O. Lame, S. Barrau, K. Ravi, F. Dalmas, Impact of carbon nanotube prelocalization on the ultra-low electrical percolation threshold and on the mechanical behavior of sintered UHMWPE-based nanocomposites. *Polymer* 111 (2017) 204-213.
- [23] E. García-Macías, R. Castro-Triguero, A. Sáez, F. Ubertini, 3D mixed micromechanics-FEM modeling of piezoresistive carbon nanotube smart concrete. *Computer Methods in Applied Mechanics and Engineering* 340 (2018) 396-423.
- [24] A.R. Alian, S.A. Meguid, Multiscale modeling of the coupled electromechanical behavior of multifunctional nanocomposites. *Composite Structures* 208 (2019) 826-835.
- [25] H. Tanabi, M. Erdal, Effect of CNTs dispersion on electrical, mechanical and strain sensing properties of CNT/epoxy nanocomposites. *Results in Physics* 12 (2019) 486-503.
- [26] X.F. Sánchez-Romate, J. Artigas, A. Jiménez-Suárez, M. Sánchez, A. Güemes, A. Ureña, Critical parameters of carbon nanotube reinforced composites for structural health monitoring applications: Empirical results versus theoretical predictions. *Composites Science and Technology* 171 (2019) 44-53.
- [27] X. Chen, A.R. Alian, S.A. Meguid, Coupled electromechanical modeling of piezoresistive behavior of CNT-reinforced nanocomposites with varied morphology and concentration. *European Journal of Mechanics - A/Solids* 84 (2020) 104053.
- [28] S.H. Jang, L.Y. Li, Self-sensing carbon nanotube composites exposed to glass transition temperature. *Materials* 13 (2020) 259.
- [29] Y. Fang, L.Y. Li, S.H. Jang, Calculation of electrical conductivity of self-sensing carbon nanotube composites. *Composites Part B: Engineering* 199 (2020) 108314.
- [30] A. Buldum, J.P. Lu, Contact resistance between carbon nanotubes. *Physical Review B* 63(16) (2001) 161403(R).
- [31] W.S. Bao, S.A. Meguid, Z.H. Zhu, Y. Pan, G.J. Weng, A novel approach to predict the electrical conductivity of multifunctional nanocomposites. *Mechanics of Materials* 46(2012) 129-138.
- [32] W.S. Bao, S.A. Meguid, Z. Zhu, Modeling electrical conductivities of nanocomposites with aligned carbon nanotubes. *Nanotechnology* 22 (2011) 485704.
- [33] W.S. Bao, S.A. Meguid, Z.H. Zhu, G.J. Weng, Tunneling resistance and its effect on the electrical conductivity of carbon nanotube nanocomposites. *J. Appl. Phys.* 111 (2012) 093726.
- [34] H. Tanabi, M. Erdal, Effect of CNTs dispersion on electrical, mechanical and strain sensing properties of CNT/epoxy nanocomposites. *Results in Physics* 12 (2019) 486-503.